Geomechanics and Engineering, *Vol. 13, No. 1 (2017) 43-61*
DOI: https://doi.org/10.12989/gae.2017.13.1.043

Evaluation of abutment types on highway in terms on driving comfort

Moon S. Nam [1a], Min-Cheol Park [*2] and Jong-Nam Do [1b]

[1] *Structure Research Division, Research Institute of Korea Expressway Corporation, 208-96, Dongbu-daero 922beon-gil, Dongtan-myeon, Hwaseong-si, Gyeonggi-do, Republic of Korea*
[2] *Department of Civil Engineering, Kumoh National Institute of Technology, 61 Daehak-ro,Gumi-si, Gyeongsnagbuk-do, Korea*

(*Received May 17, 2016, Revised February 05, 2017 Accepted February 08, 2017*)

Abstract. The inverted T-type abutments are generally used in highway bridges constructed in Korea. This type of abutment is used because it has greater stability, with more pile foundations embedded in the bedrock, while simultaneously providing support for lateral earth pressure and vertical loads of superstructures. However, the cross section of inverted T-type abutments is large compared with the piers, which makes them more expensive. In addition, a differential settlement between the abutment and embankment, as well as the expansion joints, causes driving discomfort. This study evaluated the driving comfort of several types of abutments to improve driving comfort on the abutment. To achieve this objective, a traditional T-type abutment and three types of candidate abutments, namely, mechanically stabilized earth wall (MSEW) abutment supported by a shallow foundation (called "true MSEW abutment"), MSEW abutment supported by piles (called "mixed MSEW abutment"), and pile bent and integral abutment with MSEW (called "MIP abutment"), were selected to consider their design and economic feasibility. Finite element analysis was performed using the design section of the candidate abutments. Subsequently, the settlements of each candidate abutment, approach slabs, and paved surfaces of the bridges were reviewed. Finally, the driving comfort on each candidate abutment was evaluated using a vehicle dynamic simulation. The true MSEW abutment demonstrated the most excellent driving comfort. However, this abutment can cause problems with respect to serviceability and maintenance due to excessive settlements. After our overall review, we determined that the mixed MSEW and the MIP abutments are the most appropriate abutment types to improve driving comfort by taking the highway conditions in Korea into consideration.

Keywords: inverted T-type abutments; differential settlement; driving comfort; MSEW abutment; pile bent abutment

1. Introduction

On highway bridges, the differential settlements at bridge ends (between abutments and approach slabs, as well as between abutments and embankments) can affect driving comfort, such as through rattling, and can cause safety issues (KEC 2012). Since bumps due to differential

∗Corresponding author, Postdoctoral Researcher, Ph.D., E-mail: xlage0@naver.com
[a] Deputy Principa Researcher, Ph.D., E-mail: moonsnam@gmail.com
[b] Senior Researcher, Ph.D., E-mail: donamtech@ex.co.kr

 ISSN: 2005-307X (Print), 2092-6219 (Online)

settlements at the bridge ends has become a social issue in the United States from the late 1980s, various related research and studies have been conducted by the US Department of Transportation (KEC 2012). Issues such as these have caused deterioration in driving safety, discomfort during driving, and turning of public sentiment against infrastructures such as highways. Further, these issues incur extra long-term maintenance costs and structural damage to bridges (Helwany *et al*. 2007). James and Hoffman (Briaud *et al*. 1997) reported that 25% of the bridges in the United States suffer from problems due to backfill settlements and that the maintenance costs per year reach at least approximately $100 million.

The KEC (2012) defined the settlements of embankments where abutments are located as a major cause of differential settlement at the bridge ends. Compression settlement of an embankment generates approximately 0.2% to 0.5% of the embankment height even in well-filled embankments over a long period of time. The pile foundations of abutments are generally embedded into weathered rocks and are strictly controlled in each stage of design and construction to maintain their allowable settlement to be within 10 to 25 mm. If an abutment locates at an embankment height of 20 m, the settlements of this abutment and the embankment can be calculated as 25 and 100 mm, respectively, by assuming 25 mm as the allowable settlement of piles and 0.5% of long-term compression settlement. Therefore, approximately 75 mm of differential settlement is inevitable even if the abutments and embankments are properly constructed.

To improve driving comfort by reducing the differential settlement, mechanically stabilized earth wall (MSEW) abutments were developed by supporting the abutment on MSEW, which functions as a flexible body to allow certain amount of settlements. The MSEW is a flexible structure that functions as foundations of abutments and wing wall in MSEW abutments. Thus, the differences in settlements between the abutments and embankments can be relatively small, leading to improved driving comfort (Elias *et al*. 2001). MSEW abutments have also been reported to reduce differential settlements at the approach slab connections. Experimental and numerical studies have been carried out on the structural performance and maintenance of a MSEW and MSEW abutment (Abdelouhab *et al*. 2011, Hatami and Bathurst 2006, Hossain *et al*. 2011, Huang *et al*. 2013, Kibria *et al*. 2013, Rowe and Ho 1997). The MSEW abutment is the most important structural member of the bridge, and only inextensible metallic reinforcements that exhibit relatively less lateral displacement are mainly applied (Elias *et al*. 2001). The true MSEW abutment supports the vertical load of a superstructure in a way in which the spread foundation is exploited, excessive settlement could be resulted therefrom. In addition, experimental studies and numerical analyses have been carried out for a mixed MSEW abutment employing piles to support the vertical load of a superstructure, and this resulted in an increase of their application (Huang *et al*. 2011, 2013, Pierson *et al*. 2011). Nevertheless, a quantitative analysis of the variations in driving comfort according to the settlement of reinforced earth abutment is yet to be carried out.

In addition to the application of a MSEW abutment, numerous case studies, as well as actual construction, of a new type of integral abutment bridges have focused on improving driving comfort. An integral abutment bridge is a new type of bridge that eliminates the expansion joints and integrate superstructure with substructure. The use of this type of integral abutment bridge is currently propagating rapidly in the United States and Canada (Kunin and Alampalli 2000). The superstructure of an integral abutment bridge is exposed to continuous and periodic lateral displacement via the expansion or contraction attributable to thermal variations. The lateral displacement in the superstructure would thus be supported by the integrated pile foundation, and many experimental studies and numerical analyses have been carried out on these (Arsoy *et al*.

2002, Civjan *et al*. 2007, Dicleli and Albhaisi 2003, 2004, 2015, Faraji *et al*. 2001, Fennema *et al*. 2005, Park and Nam 2007). However, integral abutment bridge that are free from expansion joints are also exposed to the differential settlement of backfill, so the variations in driving comfort resulting thereof need to be quantitatively evaluated.

The present study aims to quantitatively examine the level of driving comfort at the approach slab connections for each abutment type. Therefore, an inverted T-type abutment and other candidate abutments, namely, MSEW abutment supported by a shallow foundation (called "true MSEW abutment"), MSEW abutment supported by piles (called "mixed MSEW abutment"), and pile bent and integral abutment with MSEW (called "MIP abutment"), were selected to consider their effects on improved driving comfort and to analyze their design and economic feasibility. Finite element analysis was applied to the design section of each candidate abutment to estimate the differential settlements of the abutments as well as to provide a settlement profile of the approach slabs and embankments. On the basis of the settlement profile of each candidate abutment, the driving comfort was analyzed through a vehicle dynamic simulation analysis.

2. Selection of candidate abutment types

As flexible abutment structures that could provide improved driving comfort, the true MSEW, mixed MSEW, and MIP abutments were selected as candidates to improve driving comfort by comparing them with the traditional inverted T-type abutment, which is the most widely used abutment type in Korean highways, as shown in Fig. 1. Similar to the typical reinforced-earth retaining walls, the MSEW abutment supports lateral earth pressure of the backfill and is classified into two types, namely, true MSEW (Fig. 1(b)) and mixed MSEW (Fig. 1(c)) abutments, which support the vertical loads of superstructures with shallow and pile foundations, respectively. The MSEW abutment is known to be flexible and resistant against static and dynamic loads because it supports the vertical loads of superstructures with MSEW. In addition, this abutment type has been known to reduce costs and to be easily built (Elias *et al*. 2001, Zevgolis and Bourdeau 2007). The true MSEW abutment causes an excessive stress concentration because it supports the superstructure with direct foundations. The maximum contact pressure of the foundations on the MSEW is limited to less than 200 kPa. The mixed MSEW abutment also supports the vertical loads of a superstructure with pile foundations. However, the interactions between piles and reinforced-earth retaining walls are unclear, although research on this subject has been conducted (Huang *et al*. 2013, Pierson *et al*. 2011).

The third candidate abutment, known as the "MIP abutment" (integral abutment and pile bent separating the earth pressure by MSEW), is a mixed MSEW abutment with exterior supports and integral abutment that authors have developed. The MIP abutment supports lateral earth pressure by the MSEW, in addition to the back of the abutments and the vertical loads of the superstructure supported by pile foundations (Fig. 1(d)). In contrast to the mixed MSEW abutment, the pile foundations are constructed outside the MSEW. However, in contrast to the common externally pile-supported MSEW abutments, the MIP abutment is an integral abutment that integrates the piles and the superstructure into the abutment. Therefore, the behavior of the MIP abutment with pile foundations is identical to that of the integral abutments that support lateral displacements such as creep, shrinkage, and thermal expansion and contraction as well as the vertical loads of the superstructure with pile foundations (Arsoy *et al*. 2002, Dicleli and Albhaisi 2003, 2004, Park and Nam 2007).

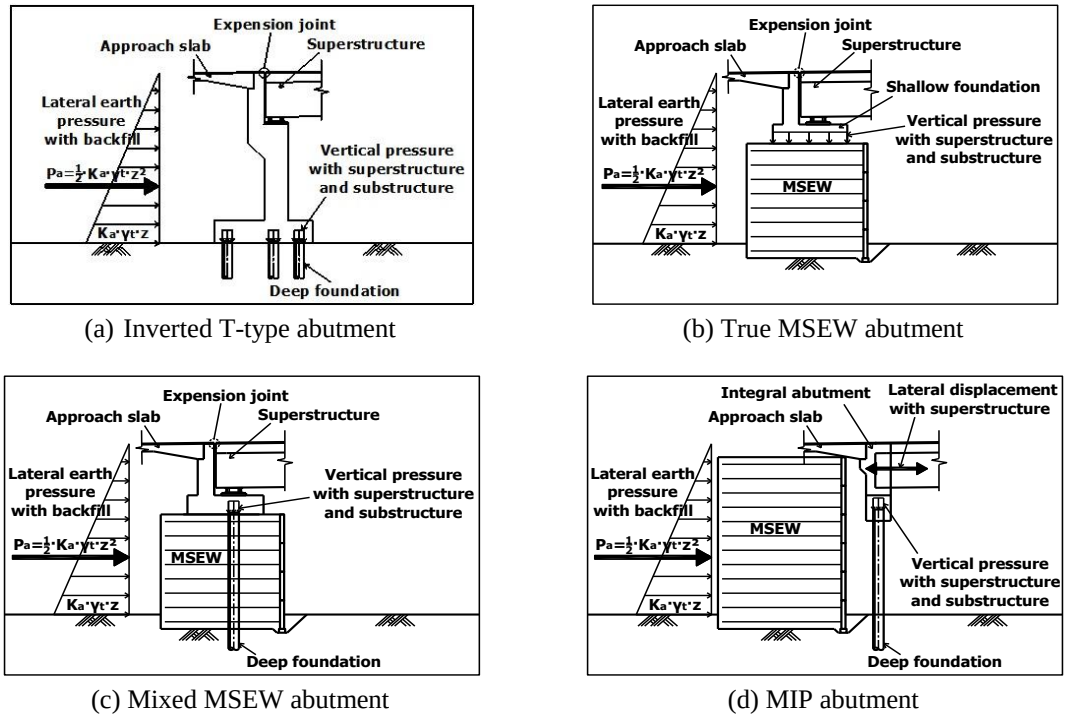

(a) Inverted T-type abutment (b) True MSEW abutment

(c) Mixed MSEW abutment (d) MIP abutment

Fig. 1 Schematics of the inverted T-type and candidate abutments

3. Review of candidate abutment design and economic feasibility

The bridge considered for the design of the candidate abutments is one of the steel box girder bridges currently used in Korean expressways. Its superstructure length, road width, and skew angle are 43.0 m, 15.6 m, and 8°, respectively. Its substructure is a 9-m-high inverted T-type concrete abutment, and both sides of the abutment are supported by wing walls and a 9-m-high block by MSEW. Hence, the economic comparison for the abutment was considered with wing walls and MSEW in this study.

The stratum consists of hard rocks, soft rocks (H = 3.8 m), weathered rocks (H = 2.0 m), colluvium (H = 9.8 m), and filled soil (H = 8.5 m) from the bottom. The bottom of the abutment is located on the filled soil and piles are penetrated into weathered rocks of approximately 1.0 m. The properties of soil and rock applied in this study was obtained from the test results performed by the KEC (2010). The properties of the geotechnical material are summarized in Table 1 that obtained from the SPT (Standard Penetration Test, KS F2307-87), PMT (Plate M Test, ASTM D 1586-11), and Piezocone Test (ASTM 3441-16) conducted by KEC (2010) at the site ground.

The design of the inverted T-type abutment was applied to the selected candidate abutments, and their design sections are shown in Fig. 2. The design conditions are as follows: the design of the inverted T-type abutment is compliant with the American Association of State Highway and Transportation Officials standard (AASHTO 2002), and the design of the MSEW abutment followed the Federal Highway Administration guidelines (Elias *et al*. 2001). The maximum ground-contact pressure of the abutment at 200 kPa and the minimum horizontal distance between the abutment and facing panel at 1.0 m comply with the design constraints. The MIP abutment is

similar to the full integral abutment in which the front fill is removed. Therefore, it complies with the design guidelines for integral abutment bridges developed by the (KEC 2010, VTrans 2008).

The inverted T-type abutment is 9.0-m high, and the lateral earth pressure is supported by the abutment, as shown in Fig. 2(a). In contrast with the gravity type abutment designed to support the lateral earth pressure with the self-weight of the concrete, the inverted T-type abutment is a structure with an improvement in external stability achieved by exploiting the weight of the embankment backfilled on its heel. However, the vertical loads of the superstructures as well as the self-weight loads of the abutments and overburden above the abutments are supported by three-row pile foundations. Thus, this abutment requires more pile foundations than the other abutments. For the pile foundation, the steel pipe pile having a diameter of 508 mm and a thickness of 12 mm was applied. It penetrated into the weathered rock by 1.0 m as an end bearing pile.The ultimate capacity determined by the static pile load test result was distributed in the range from 4,040 kN to 4,130 kN KEC (2010). The axial design capacity of the pile on the candidate abutment was 1,000 kN that was applied to take the safety factor into account. The inverted T type abutment comprised the three-row pile foundations with a length of 19.5 m, as illustrated in Fig. 2(a).

A MSEW with an inextensible reinforcement and the precast panelis used for the true MSEW (Fig. 2(b)) and the mixed MSEW (Fig. 2(c)) abutments to prevent lateral deformations. The width (b) of the metal strip employed as an inextensible reinforcement was 0.05 m, and the thicknesses were 7.0 mm (true MSEW abutment) and 5.0 mm (mixed MSEW abutment). For the true MSEW abutment, the reinforcement has to bear a heavy tensile force attributable to the vertical load of the superstructure and the lateral earth pressure of the backfilled embankment. A thickness of 7.0 mm

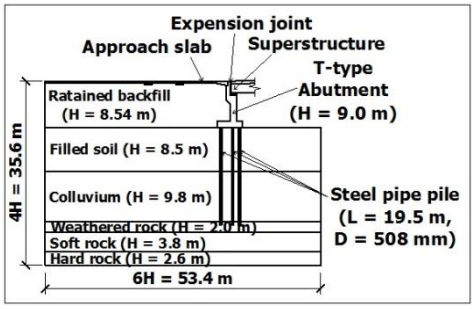

(a) Inverted T-type abutmenta

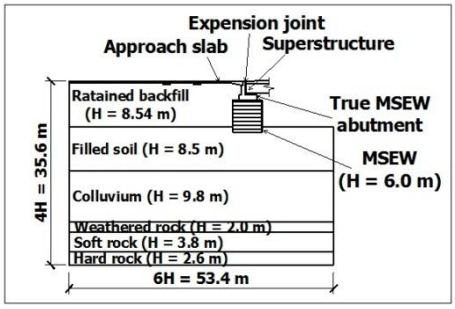

(b) True MSEW abutment

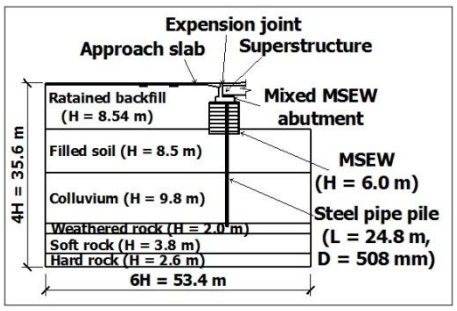

(c) Mixed MSEW abutment

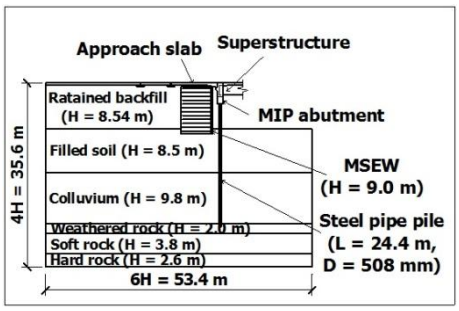

(d) MIP abutment

Fig. 2 Design section of the Inverted T-type and candidate abutments

was thus applied to improve the safety factor against a pullout and a rupture of the reinforcement. The long-term allowable tensile forces (T_d) that could take into account the thickness that corroded off after 100 years were 110.6 kN/m (true MSEW abutment) and 61.1 kN/m (mixed MSEW abutment). The external and internal stability of the MSEW abutment was examined according to the design specification, and the precast concrete panel having a width of 1.5 m and a height of 1.5 m and inextensible metal strips were thereby arranged. The lateral and vertical spacings of metal strip on the front panel were 0.5 m and 0.75 m, respectively, with 5.6 m of length (Figs. 4(a) and (b)). The axial capacity of the pile of the mixed MSEW abutment was 1,000 kN, which is equivalent to that of an inverted T type abutment, and the aligned length thereof was 24.8 m as illustrated in Fig. 2(c).

The MSEW is 6.0-m high, and the reinforcement at the back side is 5.8-m long. The true MSEW abutment supports the vertical loads of the superstructure directly to the bottom of the abutment, and the mixed MSEW abutment supports them with pile foundations. Because the true MSEW abutment is significantly affected by lateral loads inside the MSEW, an inextensible reinforcement thickness of 7 mm was used to avoid rupture, which is 2 mm thicker than that used for the mixed MSEW abutment. The MIP abutment (Fig. 2(d)) is designed to integrate the pile bent, the superstructure, and the abutment. The lateral earth pressure is supported by a 9-m-high panel-type MSEW. The pile bent foundation on the MIP abutment should be incorporated into its superstructure and should resist the lateral displacement. The member force was calculated via p-y analysis, and the expansion or contraction of the bridge attributable to the thermal variation accounted for the lateral displacement. The cross sectional of the pile was designed as a column simultaneously resist a compressive and a bending force. The design followed the process specified in the ‘Integral Abutment Bridge Design Guidelines’ (KEC 2010, VTrans 2008).

The production quantity for materials required for construction were accurately calculated based on drawings for each type of candidate abutment. In Korea, a spreadsheet (MS Excel) is frequently used to calculate the amount (area, volume) of construction materials that are required, and the construction costs were also estimated based on such calculation in order to examine the economic feasibility. To review the economic feasibility of the posterior abutment section, the construction costs were estimated using EST Plus Ver. 2.06, a commercial professional construction cost-estimation program developed by Dasansoft Co., Ltd. (Dasansoft 2014). EST Plus Ver. 2.06 easily generates the overall construction costs because it automatically calculates the costs of the construction materials, labor, and overhead required during construction for concrete, formworks, precast concrete panels, metal strip, and so on.

Fig. 3 shows the construction costs estimated using the EST. The estimated construction costs were as follows: the cost of the inverted T-type abutment was $345,000; that of the mixed MSEW

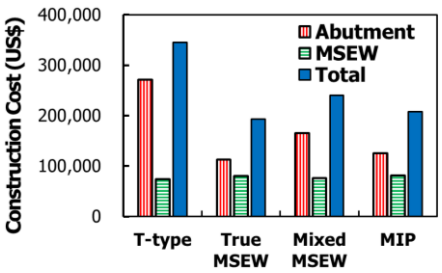

Fig. 3 Construction costs estimates for the inverted T-type and candidate abutments

abutment was $240,833, which accounted for 70% of the inverted T-type abutment cost; that of the MIP abutment was $207,500, which accounted for 60% of the inverted T-type abutment cost; and that of the true MSEW abutment was $193,333, which accounted for 56% of the inverted T-type abutment cost.

4. Driving comfort evaluation of candidate abutments

4.1 Overview of driving comfort evaluation

To evaluate the driving comfort of the candidate abutments, this study not only compared the differential settlements of the candidate abutments but also evaluated the driving comfort from the perspective of the drivers. The differential settlements at the approach slabs of the candidate abutments were calculated using finite element analysis. The driving comfort was evaluated using the differential settlements at the approach slabs of the candidate abutments. In this study, the vibrations felt by drivers while driving on the surface of the candidate abutments were analyzed using a vehicle dynamic simulation, and the degree of discomfort was quantified following international standard.

4.2 Analysis of differential settlements at the approach slabs of candidate abutments

4.2.1 Analysis overview and conditions

To analyze the differential settlements at the approach slabs of the candidate abutments and the surface settlements, the Geo-Technical Analysis System NX of MIDAS Information Technology Co., Ltd. was used to conduct the finite element analysis (MIDAS 2013).

(1) Boundary conditions and geometry

The candidate abutment types are complex structures that consist of concrete abutments, pile

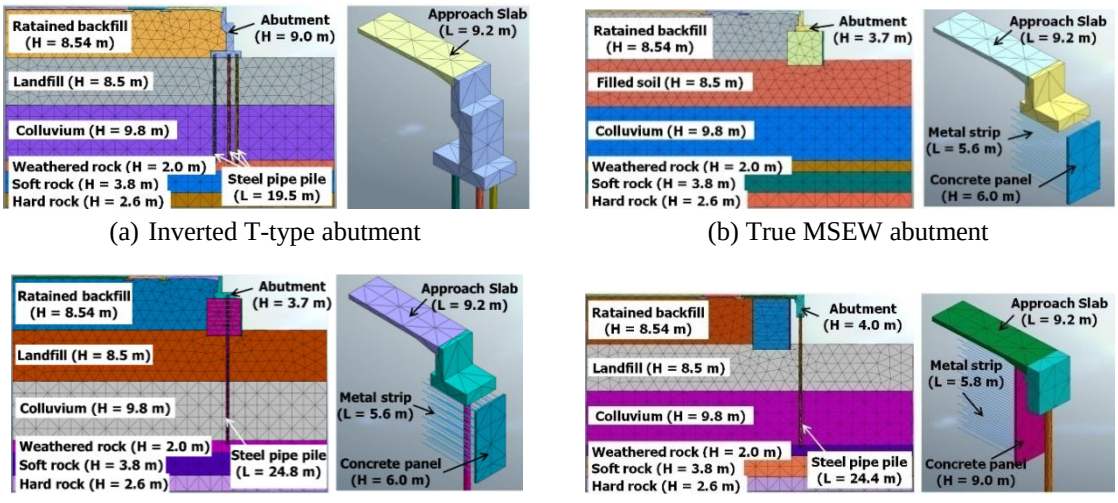

(a) Inverted T-type abutment (b) True MSEW abutment

(c) Mixed MSEW abutment (d) MIP abutment

Fig. 4 Geometries of the inverted T-type and candidate abutments

foundations, reinforced-earth retaining walls, and approach slabs. To evaluate their performance, the finite element analysis must be efficiently and accurately conducted. The geometry of the finite element analysis is basically the same as the blueprint shown in Fig. 4. In order to avoid the interference with piles and inextensible reinforcements in the mixed MSEW abutment, three-dimensional finite element analyses were conducted in this study rather than two-dimensional finite element analyses. However, it takes a long time to analysis for the whole modeling of the abutment and the neighboring ground condition in three dimensions. To solve this problem, the abutment width was modeled as a unit width of 3.0 m considering an appropriate distance between the pile and the inextensible reinforcement. The influential range of the pile foundation, usually 2.5 times a pile diameter, and a horizontal spacing of 0.5 m for the metal strip were taken into account to create geometries with a unit width of 3.0 m along the y-direction. The applicability of the model in the finite element analysis employing the geometries with a unit width of 3.0 m was verified by comparing its results with those obtained from a static pile load test conducted by (KEC 2010). The verification of model was carried out using the axial load-settlement curve, as illustrated in Fig. 6.

The bottom of the model is restrained in the *x*, *y* and *z* directions and the right and left sides of the model are restrained in the y direction. The front and back side of model are restrained in the *x* direction.

(2) Analysis methods and procedure

Nonlinear elasto-plastic analyses were carried out to calculate the settlement for each type of candidate abutment. Based on the construction procedure prepared during the design of the candidate abutments, the corresponding stages of the finite element analyses were developed. In the first stage, the piles were formed before initializing stress conditions. Then, the displacement was initialized to calculate the initial stress of the in-situ ground. The initial stress of the in-situ ground as k0 condition was calculated after the piles were installed because the piles are pre-bored in-placed piles. The second stage shows the construction of the abutments. Because the main purpose of this study was to compare the driving comfort of the various abutment types, construction details such as backfilling procedures behind abutments and the influence of ground water and pore pressure were not considered in this study to simplify the analysis. In the third stage, the construction of the structural members of the road surface and embankments was completed. In the fourth stage, the vertical load of 160.0 kPa for the superstructure was based on the results obtained from structural analyses conducted by (KEC 2010), and the vehicle load of 12.7 kPa was borrowed from that of the DL-24 class presented in AASHTO (2002).

(3) Element model and properties

The geotechnical model for the finite element analysis considered a 4 noded tetrahedron, and the Mohr–Coulomb model was applied. In general, a soil model for the MSEW with the extensible reinforcement, which induces relatively large displacements, mostly uses a hyperbolic model proposed by Hatami and Bathurst (2006), and the hyperbolic model proposed by Hatami and Bathurst (2006) and the Mohr-Coulomb model shows similar behavior within an elastic condition. Huang *et al*. (2009) employed three different continuum models (the Mohr-Coulomb model, Duncan-Chang model, and Lade model) to conduct numerical analyses for the MESW with a precast concrete panel and an inextensible reinforcements. The Mohr-Coulomb model exhibited complete plastic behaviors from a comparison with the results obtained from the triaxial compression test while the Duncan-Chang model and Lade model appeared reflecting ductile

behaviors resulting from the triaxial compression test. Based on Huang *et al*. (2009), the difference in the displacement of the precast concrete panel due to the surface load appeared to be insignificant among the three models. Since the candidate abutments for each type behave in the elastic region by the optimized design, the Mohr-Coulomb model was applied to the ground element.

Table 1 lists the summary of the properties of the geotechnical characteristics, which were estimated from the results of ground investigation of applicable bridges conducted by the KEC (2010). In the reference material provided by KEC (2010), SPT (Standard Penetration Test, KS F2307-87), PMT (Plate M Test, ASTM D 1586-11), and piezocone test (ASTM 3441-16) were carried out at the site ground to calculate the elastic modulus and Poison's ratio for the filled soil, alluvial, weathered rock, soft rock, and hard rock. The total unit weight, internal friction angle, and

Table 1 Properties of geotechnical characteristics

	γ_t (kN/m^3)	K_0	Linear-elastic model		Mohr-coulomb plastic model			
			$E\ (kPa)$	υ	ϕ (°)	ψ (°)	$c\ (kPa)$	$T_s\ (kPa)$
Retained backfill	19.0	0.5	90,000	0.30	35	5	10	10
Reinforced backfill	19.0	0.5	100,000	0.30	35	5	10	10
Landfill	19.0	0.5	77,300	0.35	35	0	10	1
Colluvium	19.0	0.5	84,500	0.30	35	0	10	1
Weathered rock	20.0	0.5	210,000	0.35	35	1	20	50
Soft rock	24.0	1.0	735,000	0.20	40	2	50	50
Hard rock	27.0	1.0	4,590,000	0.20	45	10	100	50

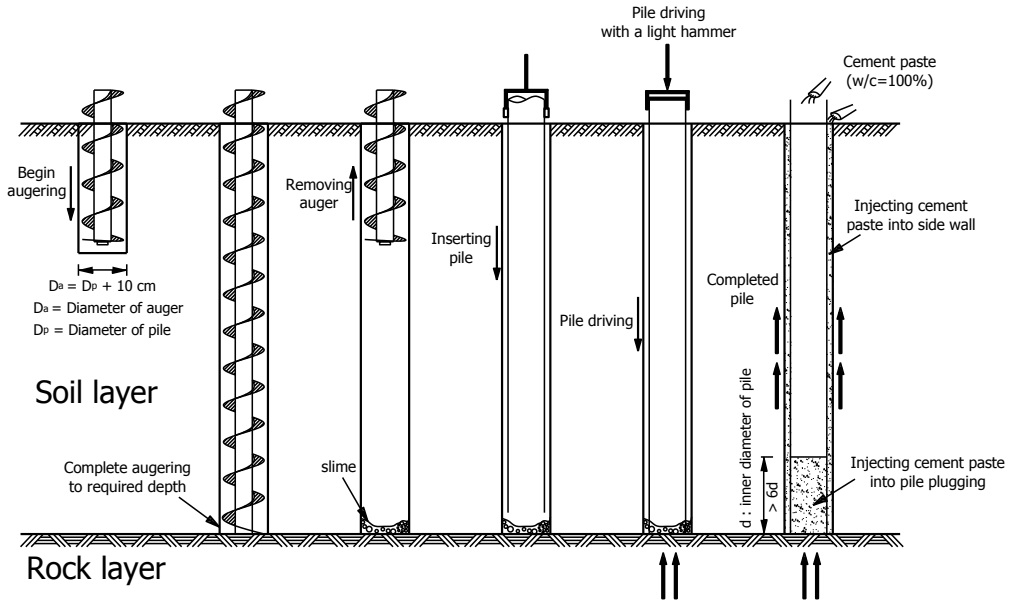

Fig. 5 Construction procedure of the pre-boringin-placed piling method

cohesion were estimated by applying the results of the site investigation and the representative values used in South Korea. The dilatancy angle was calculated based on the construction that followed the 'pre-bored in-placing precast piling method' conducted by (KEC 2010). As the piles were constructed using the pre-boring in-placed piling method (Fig. 5), the soil under the confining pressures were released during the pre-boring, and the volume of the nearby soil increased. Because the volumes of the land fill and the colluvium increased during the pre-boring, a dilatancy angle of 0° was applied. A dilatancy angle of 1° was applied to the weathered soil around the pile toes, and a dilatancy angle of 5° was applied to the MSEW and embankments.

The other properties of the embankment and reinforced earth were calculated by considering the results of the numerical analyses conducted by Abdelouhab *et al*. (2011) on the panel-type MSEW as well as the banking and compaction standards of KEC (2012). As was pointed out by Potts (2003), the calculation for the post-yield plastic deformation conducted through a numerical analysis is distinguished into the associated flow rule and the non-associated flow rule. The associated flow rule would be used when the dilatancy angle corresponds to the internal friction angle. Otherwise, the calculation would be completed by following the non-associated flow rule (Kim *et al*. 2009a, Kim *et al*. 2009b). Sandy soil has been well known to follow the non-associated flow rule (Rahim 1998). In this study, the value of the dilatancy angle of the panel-type reinforced earth retaining wall was calculated to be smaller than that of the internal friction angle, as is shown in Table 1 by referring to the results of the study conducted by Abdelouhab *et al*. (2011).

The structural members of the candidate abutments and piles were divided into concrete and steel materials, and the summary of their properties is listed in Table 2. The concrete material used for the abutments, the facing panels of the MSEW, approach slabs, connection slabs, and sleeper slabs and were modeled using a 4 noded tetrahedron, similar to that of the ground, and the linear elastic model was applied. The steel materials included steel-pipe piles and metal strips of the MSEW. The steel-pipe piles with a diameter of 508 mm and a thickness of 12 mm were modeled using a 4 noded tetrahedron, and the von Mises yield model was applied (Chung *et al*. 2010, Kim *et al*. 2009a, Kim *et al*. 2009b). The geometry of inextensible reinforcement was created as a 2-dimensional object as a line, with the truss element solely bearing the axial load. The Tresca model that is generally used for steel materials was employed as the model of inextensible reinforcement, and the elastic coefficient and yield strength thereof were referred to in the paper by Zevgolis and Bourdeau (2007).

(4) Boundary condition between ground and structure

The candidate abutments for each type consist of the structural and the geotechnical members that create interactions with each other. The interaction between the soil/rock and structure greatly affects the results of the finite element analyses. In this study, Zero-thickness interface elements were applied to the interface between the structural and the geotechnical (Comodromos and Pitilakis 2005, Fellenius 2004, Huang *et al*. 2013, Pierson *et al*. 2011). The Coulomb friction

Table 2 Structural characteristics

	γ_t	Linear-elastic model		Non-linear model
	(kN/m^3)	$E\ (MPa)$	υ	$\sigma_y\ (kPa)$
Concrete	25.0	27,000	0.17	-
Steel pipe pile	77.0	153,200	0.30	250,000
Metal strip	76.8	210,000	0.27	450,000

model was applied to reproduce the separation and sliding at the interface between the structural members and the ground (Table 3).

In particular, the performance of the abutments was determined by the performance of the piles supporting the vertical loads of the superstructures. To simulate such performance, the behavior of the interface between the piles and ground must dominantly work. Thus, the properties of the interface between the piles and soil and the rock were determined by studying the parameters according to the results from the field load tests of a single pile done performed by the KEC (2010). The results are shown in Fig. 6. In addition, a previous work has shown that the point bearing of the deep foundation does not have a limiting value and continues to increase, depending on the displacement (Fellenius 2004). An expansion angle was applied to practically simulate the increased strength using volume expansion after the yielding point (Potts 2003).

The interface properties between the piles and the soil/rock presented in Table 3 were calculated through a comparative verification of the results obtained from the field load test, as represented in Fig. 6. Next, the value of the interface between the metal strip and ground, and that between the concrete and ground, were calculated using the following formula(s). In general, the normal stiffness modulus (k_n) and tangential stiffness modulus (k_t) of the interface are determined by the stiffness of the adjacent ground. Eq. (1) was used to calculate the normal stiffness modulus (k_n) while Eq. (2) was employed to calculate the tangential stiffness modulus (k_t).

$$k_n = \frac{E_{oed,i}}{L \times t_v} \tag{1}$$

$$k_t = \frac{G_i}{L \times t_v} \tag{2}$$

Table 3 Structure-soil interface characteristics

	Structural parameters		Nonlinear - coulomb friction model			
	k_n (kN/m^3)	k_t (kN/m^3)	c (kPa)	ϕ (°)	ψ (°)	T_s (kPa)
Pile - soil	210,000	100,000	10	25	4	100
Metal strip - soil	343,200	31,200	6	21	0	10
Concrete - soil	228,800	20,800	8	28	0	10

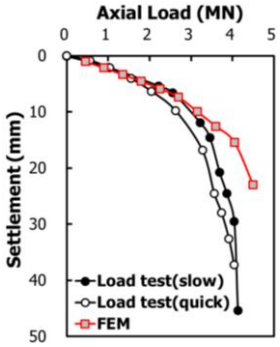

Fig. 6 Back analysis usingfield load test to estimate the proper interface property

where, $E_{oed,i}$: elastic coefficient in kPa derived from an oedometer test with a value calculated by using Eq. (3).

$$E_{oed,i} = 2 \times G_i \times \left\{ \frac{(1 - v_i)}{(1 - 2 \times v_i)} \right\} \tag{3}$$

L : an unit length of the inextensible reinforcement to which a value of 1.0m was applied by taking the size of the truss element into account.

t_v : a virtual thickness generally ranging from 0.01 to 1.0 (MIDAS 2013) wherein smaller values would be applied in accordance with an increasing difference in the stiffness between the adjacent elements.

v_i : a Poisson's ratio for the interface introduced to simulate the incompressible frictional behavior, to which a value of 0.45 was automatically applied to prevent numerical errors.

G_i : a shear modulus of elasticity of 1.0 was applied in this study, and its value is calculated using Eq. (4).

$$G_i = R \times G_{soil} \tag{4}$$

R : a general strength reduction factor dependent on the characteristics of the structural members and adjacent soil. In general, the values used are $R = 0.6 \sim 0.7$ for sandy soil and steel materials, $R = 0.5$ for clay and steel materials, $R = 1.0 \sim 0.8$ for sandy soil and concrete, and $R = 0.7 \sim 1.0$ for clay and concrete (MIDAS 2013). The value of 0.6 for the strength reduction factor was employed for the interface between the metal strip and soil whereas a value of 0.87 was applied to the interface between concrete and ground.

G_{soil} : a shear modulus of the soil in kPa and it is calculated as expressed in Eqs.(5).

$$G_{soil} = \frac{E_{soil}}{2(1 + \nu_{soil})} \tag{5}$$

4.2.2 Analysis results

The amount of settlement at the abutments, backfills, and embankments was calculated by finite element analysis, and the differential settlements between the abutments, backfills, and embankments were estimated as follows:

(1) Displacement of abutment and the ground at the back of the abutment

The settlements on the ground at the back of the abutments cause differential settlements at the approach slabs and eventually result in deterioration in the driving comfort, serviceability, and performance of the entire bridge. The displacement diagram obtained from the finite element analysis is shown in Fig. 7, which compares the displacement of the abutment, backfill, and embankment induced by the vertical loads of the superstructures and vehicles. Because the three-row piles support the inverted T-type abutment, its settlement was calculated to be relatively smaller than that of the other abutment types. Accordingly, the relative differential settlement between the abutment, backfill, and embankment was the largest at 30.2 mm (Fig. 7(a)). The true MSEW abutment supported the vertical loads of the superstructure with the MSEW, which are flexible structures. Therefore, its settlement was calculated to be relatively larger than those of the other types (Fig. 7(b)). Thus, the relative differential settlement between the abutment, backfill, and embankment was found to be the smallest at 2.9 mm. In contrast to the true MSEW abutment, the mixed MSEW and MIP abutments supported the vertical loads of the superstructures with pile foundations. Thus, the amount of abutment settlement was calculated to be relatively small, and

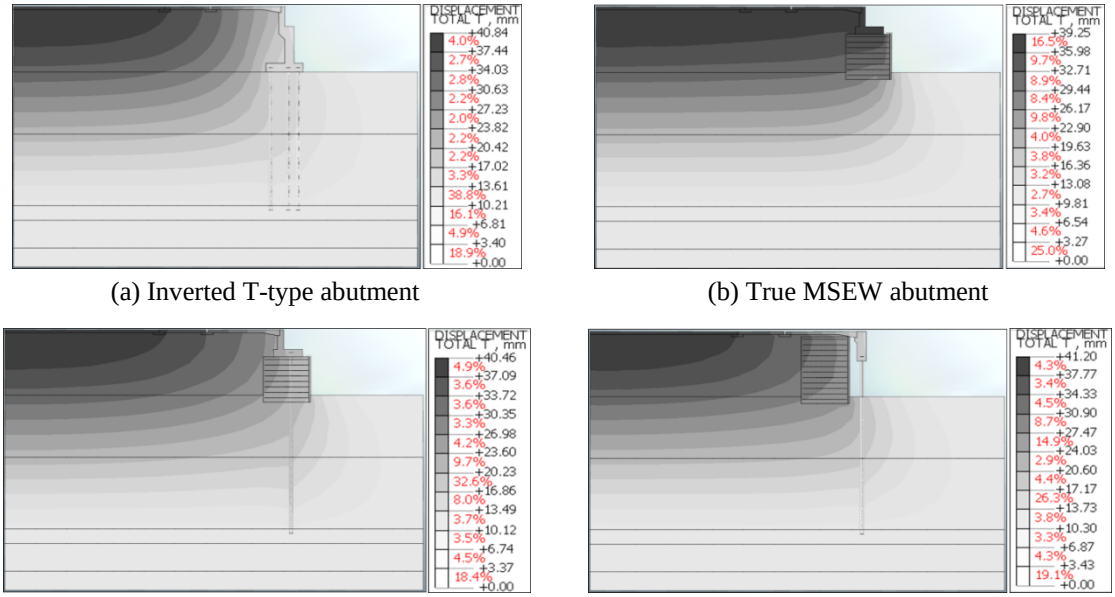

(a) Inverted T-type abutment (b) True MSEW abutment

(c) Mixed MSEW abutment (d) MIP abutment

Fig. 7 Displacement diagram of the inverted T-type and candidate abutments

the differential settlements between the abutment, backfill, and embankment were 20.3 and 28.2 mm (Figs. 7(c) and (d)). They had to support the vertical loads of the superstructures with one-row piles, which are fewer than the three-row piles of the inverted T-type abutment. Accordingly, the level of abutment settlement was relatively high.

(2) Comparison of the differential settlements at the approach slab connection

To identify the differential settlements between the abutment, backfill, and embankment of the candidate abutments, the settlements of abutments as well as the amount of settlement at the approach slabs, relief slabs, and on the paved road surface are shown in Figs. 8 and 9. For the settlements of the abutments, the displacement at the bridge bearing was considered, as shown in Fig. 8. The displacement of the inverted T-type abutment was 10.6 mm, the true MSEW abutment was 36.3 mm, the mixed MSEW abutment was 20.1 mm, and the MIP abutment was 15.2 mm.

Because the true MSEW abutment supported the vertical loads of the superstructure with a shallow foundation on the MSEW, settlements of the backfill, embankment, and MSEW simultaneously occurred. Thus, the displacement at the bridge bearing appeared to be the largest, exceeding the generally used allowable settlement of 25.4 mm. Since an allowable vertical displacement of the MSEW is generally used 1.0 per cent of its height, the allowable vertical settlement for the true MSEW abutment is 60 mm. The vertical estimated displacement of the true MSEW abutment was within the allowable range in point of the MSEW. However, it could be exceeded the allowable range in point of the bridge structure itself.

Because the mixed MSEW and MIP abutments were supported by a one-row pile foundation, the vertical loads of the superstructure on each pile were larger than those of the inverted T-type abutment supported by a three-row pile foundation. Therefore, the settlements of the mixed MSEW and MIP abutments were larger than that of the inverted T-type abutment. In contrast to the

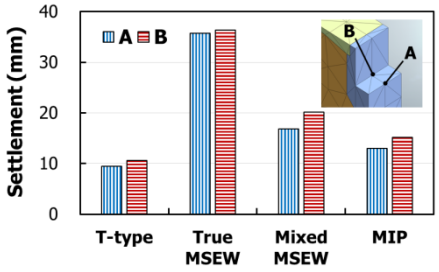

Fig. 8 Displacement of the bridge bearings

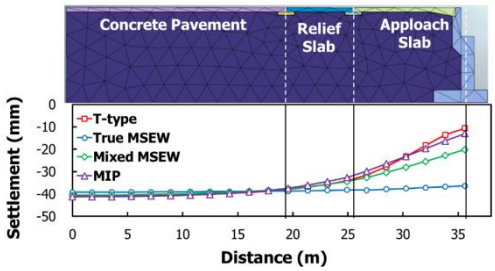

Fig. 9 Settlement profile on the road surface for each abutment

MIP abutment, the mixed MSEW abutment contained piles inside the MSEW, which means that the displacement was relatively large due to the self-weight loads and the own settlement of the MSEW abutment.

The amounts of settlement of the abutment candidates, approach slabs, relief slabs, and paved road surfaces were compared and shown in Fig. 9. The settlement of the true MSEW abutment was nearly identical. As a result, a differential settlement of 2.94 mm barely occurred. The inverted T-type, mixed MSEW, and MIP abutments supported by the piles generated the biggest differential settlements at the approach slabs, which were 20.9, 12.5, and 16.8 mm, respectively. The settlement profiles of the abutments, approach slabs, and road surfaces of the candidate abutments obtained from the finite element analysis were applied to the vehicle dynamic simulation to evaluate the driving comfort.

4.3 Evaluation of driving comfort at the approach slab connection for each candidate abutment

4.3.1 Overview of the driving comfort analysis

The driving comfort of each candidate abutment was analyzed using the settlement profiles of the abutments, approach slabs, and road surfaces calculated through the finite element analysis. To analyze the driving comfort, CarSim 9.0.3, a dynamic motor-vehicle driving analysis program developed by Mechanical Simulation Corporation, was used for the vehicle dynamic simulation to calculate the vibration acceleration felt by the drivers. The CarSim software allows users to conduct a simulation analysis of the dynamic behavioral characteristics of vehicles through a computer. This program provides users with a three-dimensional road at which vehicle dynamic simulation and analysis of different types of vehicles are available (Fig. 10) (MSC 2014).

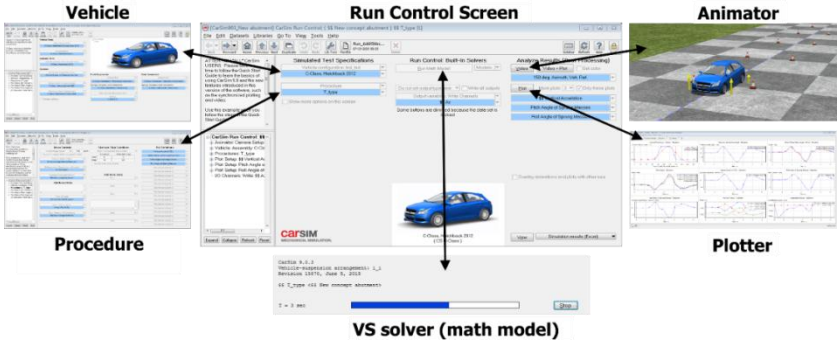

Fig. 10 Schematic of CarSim analysis

The road topography used in the driving comfort analysis was created using the settlement profiles of the candidate abutments calculated through the finite element analysis. To minimize the effects of dynamic characteristics at the approach slabs, which depend on the acceleration or deceleration of vehicles, a sufficient distance of more than 100 m from the approach slab connection was allowed for the acceleration or deceleration of vehicles (Fig. 11). The vehicle employed in the dynamic simulation was driven around the approach slab connection of the candidate abutments at the speeds of 60-140 km/h to analyze the driving comfort while entering onto or exiting from the approach slab connection. A C-class vehicle whose wheelbase was 2.91 m and height was 1.61 m was used for the analysis. This vehicle was driven on the road for each candidate type to calculate the acceleration in the z-direction that most significantly affects the differential settlements at the approach slabs using the triaxial acceleration created during driving (Fig. 11).

The evaluation of the acceleration using the differential settlements at the approach slabs obtained by the vehicle dynamic simulation was performed in accordance with the Mechanical Vibration and Shock-Evaluation of Human Exposure to Whole-Body Vibration of ISO2631 (ISO 1997). ISO 2361 establishes methods of evaluating the physical reaction of drivers against mechanical vibration or impact. ISO 2361 has been determined to be the most appropriate quantitative method in evaluating the vibration acceleration of a vehicle in a vehicle dynamic simulation depending on the differential settlements at the approach slabs. ISO 2361 recommends the use of root mean square (RMS) values, which evaluate the acceleration measured from the vibration or impact of vehicles, as expressed in Eq. (6). According to the RMS values, the degree

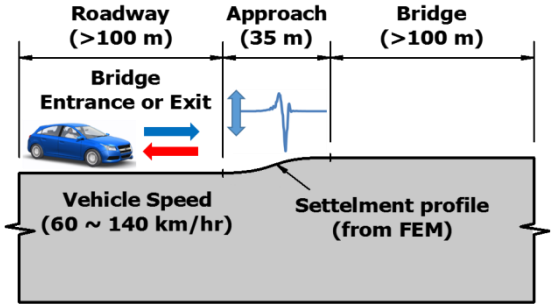

Fig. 11 Road geometry and procedure in CarSim analysis

Table 4 Comfort ratingrelative to vibration environments

RMS (m/s^2)	Ratings
Less than 0.315	Not uncomfortable
0.315 to 0.63	A little uncomfortable
0.5 to 1.0	Fairly uncomfortable
0.8 to 1.6	Uncomfortable
1.25 to 2.5	Very uncomfortable
Greater than 2	Extremely uncomfortable

of inconvenience felt by drivers resulting from vibration was divided into six stages, as listed in Table 4.

$$RMS = \left[\frac{1}{T}\int_0^T a_w^2(t)dt\right]^{1/2} \tag{6}$$

Where, a_w (t) is the frequency-weighted acceleration at time t and T is the measurement time.

In this study, the settlement profile of the abutment, approach slab, relief slab, and embankment of each abutment type, which was obtained using the finite element analysis, was applied to CarSim to conduct a vehicle dynamic simulation. As a result, the acceleration in the z-direction depending on the driving speeds and direction was calculated. In accordance with ISO 2631, the RMS value was calculated using the acceleration of the vehicle driven on the candidate abutments to evaluate the driving comfort in each abutment.

4.3.2 Results of the driving comfort evaluation

Fig. 12 shows the driving speeds and results of the RMS values at the times when the vehicle entered onto and exited from each candidate abutment. When the vehicle entered onto the abutment, the RMS value was slightly larger than that when the vehicle exited from the abutment. In addition, the RMS value increased as the driving speed increased. The RMS value of the inverted T-type abutment with the largest difference in settlement, which was the value obtained using the finite element analysis, was the largest. The true MSEW abutment showed the most excellent driving comfort as the driver did not feel any discomfort in all driving speed conditions.

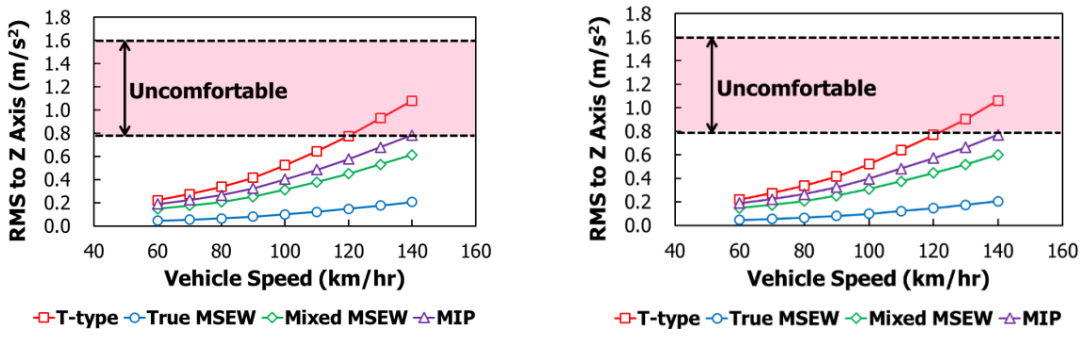

(a) Entrance condition (b) Exit condition

Fig. 12 Driving discomfort according to the entrance and exit conditions for each abutment

The RMS values of the candidate abutment types were compared. The drivers felt "fairly uncomfortable" while they were driving on the inverted T-type abutment at a speed of 100 km/h or faster. In particular, the drivers felt "uncomfortable" while they were driving on the inverted T-type abutment at a speed of 120 km/h or faster. The drivers felt "fairly uncomfortable" while they were driving on the MIP abutment at a speed of 120 km/h or faster and on the mixed MSEW abutment at a speed of 130 km/h or faster.

A trend toward higher speed limits has appeared on the highways in Korea, prompted by the recent building of the so-called "smart highway." In addition, the driving comfort of passengers must be considered. In consideration of the aforementioned factors, the inverted T-shaped abutment is determined to be inappropriate for Korean highways.

5. Conclusions

This study intended to identify the problems of differential settlements and driving discomfort on inverted T-type abutments, which have been widely used in Korean highways. Furthermore, to improve driving comfort, some candidate abutment types were selected to quantitatively analyze the effectiveness on improved driving comfort. Therefore, the economic feasibility of each candidate abutment was assessed through investigation of the design and driving comfort, which were evaluated through finite element analysis and vehicle dynamic simulation. The conclusions are summarized as follows:

(1) The design of each candidate abutment was reviewed. The inverted T-type abutment needed to resist more earth pressure and vertical loads than the other candidate abutments because of its bulky section, which requires more pile foundations than the other abutments. Because the pile foundations of the inverted T-type abutment are generally embedded more than 1 m into weathered rocks strictly controlled by the allowable settlement of 25.4 mm, significant differential settlements with the backfill and the embankment of the abutment resulted, where a long-term compression settlement occurs. Supporting vertical and lateral loads by the MSEW, which are flexible structures, was considered to be an effective alternative to reduce differential settlements between the abutment, backfill, and embankment.

(2) Each candidate abutment was analyzed using finite element analysis. The displacement at the bridge bearing of the inverted T-type abutment supported by three-row pile foundations was found to be the smallest, and the relative differential settlement between the backfill, embankments, and abutment was the largest. The displacement at the bridge bearing of the true MSEW abutment was the largest, whereas the relative differential settlement between the backfill, embankments, and abutment was the smallest. However, the excessive displacement at the bridge bearing was caused by the excessive vertical loads from the top of the MSEW.

(3) The driving comfort of each candidate abutment was evaluated. The RMS value at the time when the vehicle entered onto the abutment was slightly larger than that when the vehicle exited from the abutment. Furthermore, as the driving speed increased, the RMS value remarkably increased. The RMS value of the inverted T-type abutment, whose relative difference in settlement was the largest, appeared to be the largest. The driver did not feel any discomfort in all speed conditions on the true MSEW abutment, which indicated that this type provided the most excellent driving comfort.

(4) The driver felt "fairly uncomfortable" while driving on the inverted T-type abutment at a speed of 100 km/h or faster. In particular, the driver felt "uncomfortable" while driving on the inverted T-type abutment at a speed of 120 km/h or faster. The driver also felt "fairly uncomfortable" while driving on the MIP abutment at a speed of 120 km/h or faster and on the mixed MSEW abutment at a speed of 130 km/h or faster.

(5) The result of this comprehensive evaluation of driving comfort showed that the true MSEW abutment provided the most excellent driving comfort. This result was attributed to a relatively small differential settlement at the bridge ends, which came from the good settlement of the abutment supported by the flexible MSEW body. Therefore, the true MSEW abutment could cause maintenance problems, and the bridge would bear differential settlements prompted by excessive settlements.

(6) A trend toward higher speed limits has occurred on the highways in Korea, prompted by the recent building of the so-called "smart highway." In addition, the driving comfort of passengers must be considered. In consideration of these factors, the inverted T-shaped abutment was determined to be inappropriate for Korea highways. The true MSEW abutment, which provides the most excellent driving comfort, could cause problems in terms of serviceability and maintenance due to excessive displacement at the bridge bearing. Therefore, when Korean highway conditions are considered, the mixed MSEW and MIP abutments are determined to be the most appropriate abutment types to improve driving comfort as well as in terms of proper maintenance.

References

AASHTO (2002), Standard Specifications for Highway Bridges; 17th Edition.

Abdelouhab, A., Dias, D. and Freitag, N. (2011), "Numerical analysis of the behaviour of mechanically stabilized earth walls reinforced with different types of strips", *Geotext. Geomembr.*, **29**(2), 116-129.

Arsoy, S., Barker, R.M. and Duncan, J.M. (2002), "Experimental and analytical investigations of piles and abutments of integral bridges", Virginia Department of Transportation, pp. 1-55.

Briaud, J.L., James, R.W. and Hoffman, S.B. (1997), "Settlement of bridge approaches: (the bump at the end of the bridge); NCHRP Synthesis 234", Transportation Research Board, Washington, D.C., USA, pp. 1-81.

Chung, M.-K., Lee, S.-H., Lee, J.-H., Kwak, K.-S. and Kim, S.-R. (2010), "Reinforcement Effect of Steel-Concrete Composite Group Piles by Numerical Analysis", *J. Korean Geotech. Soc.*, **26**(11), 29-38.

Civjan, S.A., Bonczar, C., Brena, S.F., DeJong, J. and Crovo, D. (2007), "Integral abutment bridge behavior: Parametric analysis of a Massachusetts bridge", *J. Bridge Eng.*, **12**(1), 64-71.

Comodromos, E.M. and Pitilakis, K.D. (2005), "Response evaluation for horizontally loaded fixed-head pile groups using 3-D non-linear analysis", *Int. J. Numer. Anal. Method. Ingeomech.*, **29**(6), 597-625.

Dasansoft (2014), EST Plus user manual; Dasansoft Co. Ltd., Korea.

Dicleli, M. and Albhaisi, S.M. (2003), "Maximum length of integral bridges supported on steel H-piles driven in sand", *Eng. Struct.*, **25**(12), 1491-1504.

Dicleli, M. and Albhaisi, S.M. (2004), "Effect of cyclic thermal loading on the performance of steel H-piles in integral bridges with stub-abutments", *J. Constr. Steel Res.*, **60**(2), 161-182.

Dicleli, M. and Erhan, S. (2015), "Low cycle fatigue effects in integral bridge steel H-piles under earthquake induced strain reversals", *Adv. Struct. Eng.*, Springer, 2505-2512.

Elias, V., Barry, P. and Christopher, R. (2001), "Mechanically Stabilized Earth Walls and Reinforced Soil Slopes Design and Construction Guidelines", US Department of Transportation; Federal Highway Administration, Washington, D.C., USA, pp. 1-394.

Faraji, S., Ting, J.M., Crovo, D.S. and Ernst, H. (2001), "Nonlinear analysis of integral bridges: finite-element model", *J. Geotech. Geoenviron. Eng.*, **127**(5), 454-461.

Fellenius, B.H. (2004), "Unified design of piled foundations with emphasis on settlement analysis: Current Practices and future trends in deep foundations", *Proceedings of Geo-Trans Conference*, Los Angeles, USA, pp. 253-275.
Fennema, J.L., Laman, J.A. and Linzell, D.G. (2005), "Predicted and measured response of an integral abutment bridge", *J. Bridge Eng.*, **10**(6), 666-677.
Hatami, K. and Bathurst, R.J. (2006), "Numerical model for reinforced soil segmental walls under surcharge loading", *J. Geotech. Geoenviron. Eng.*, **132**(6), 673-684.
Helwany, S., Koutnik, T.E. and Ghorbanpoor, A. (2007), "Evaluation of bridge approach settlement mitigation methods", University of Wisconsin-Milwaukee, pp. 1-113.
Hossain, M., Kibria, G., Khan, M., Hossain, J. and Taufiq, T. (2011), "Effects of backfill soil on excessive movement of MSE wall", *J. Perform. Constr. Facil.*, **26**(6), 793-802.
Huang, B., Bathurst, R.J. and Hatami, K. (2009), "Numerical study of reinforced soil segmental walls using three different constitutive soil models", *J. Geotech. Geoenviron. Eng.*, **135**(10), 1486-1498.
Huang, J., Parsons, R.L., Han, J. and Pierson, M.C. (2011), "Numerical analysis of a laterally loaded shaft constructed within an MSE wall", *Geotext. Geomembr.*, **29**(3), 233-241.
Huang, J., Han, J., Parsons, R.L. and Pierson, M.C. (2013), "Refined numerical modeling of a laterally-loaded drilled shaft in an MSE wall", *Geotext. Geomembr.*, **37**, 61-73.
ISO (1997), Mechanical vibration and shock-Evaluation of human exposure to whole-body vibration-Part 1: General requirements, ISO 2631-1; International Organization for Standardization.
KEC (2010), Practical Application of Semi-integral abutment bridge; Expressway & Transportation Research Institute, Korea.
KEC (2012), Evaluation and Improvement of Ride Discomfort at Bridge Approaches in Service; Express-way & Transportation Research Institute, Korea.
Kibria, G., Hossain, M.S. and Khan, M.S. (2013), "Influence of soil reinforcement on horizontal displacement of MSE wall", *Int. J. Geomech.*, **14**(1), 130-141.
Kim, S.-R., Lee, J.-H., Park, J.-H. and Chung, M.-K. (2009a), "Analysis of reinforcement effect of steel-concrete composite piles by numerical analysis (I) - Material strength", *J. Korean Soc. Civil Engr.*, **29**(6C), 259-266.
Kim, S.-R., Lee, S.-H., Chung, M.-K. and Lee, J.-H. (2009b), "Analysis of reinforcement effect of steel-concrete composite piles by numerical analysis (II) - Bearing capacity", *J. Korean Soc. Civil Engr.*, **29**(6C), 267-275.
Kunin, J. and Alampalli, S. (2000), "Integral abutment bridges: current practice in United States and Canada", *J. Perform. Constr. Facil.*, **14**(3), 104-111.
MIDAS, I.T. (2013), GTS NX on-line manual; MIDAS Information Technology Co., Ltd., Korea.
MSC (2014), CarSim Quick Start Guide; Mechanical Simulation Corporation, USA.
Park, Y.H. and Nam, M.S. (2007), "Behavior of earth pressure and movements on integral abutments", *J. Korean Soc. Civil Engr.*, **27**(3C), 163-173.
Pierson, M.C., Parsons, R.L., Han, J. and Brennan, J.J. (2011), "Laterally loaded shaft group capacities and deflections behind an MSE wall", *J. Geotech. Geoenviron. Eng.*, **137**(10), 882-889.
Potts, D.M. (2003), "Numerical analysis: A virtual dream or practical reality?" *Geotechnique*, **53**(6), 535-573.
Rahim, A. (1998), "The significance of non-associated plasticity", *Crisp News*, Issue 6.
Rowe, R.K. and Ho, S. (1997), "Continuous panel reinforced soil walls on rigid foundations", *J. Geotech. Geoenviron. Eng.*, **123**(10), 912-920.
VTrans, I.A.C. (2008), Integral Abutment Bridge Design Guidelines; (2nd Ed), VTrans Structures Section, The State of Vermont, Agency of Transportation, Montpelier, VT, USA.
Zevgolis, I. and Bourdeau, P. (2007), "Mechanically stabilized earth wall abutments for bridge support", Joint Transportation Research Program; Indiana Department of Transportation and Purdue University, Indiana, pp. 1-146.